IOP Conference Series: Materials Science and Engineering



# Efficiency Enhancement of Dye-Sensitized Solar Cells (DSSCs) using Copper Nanopowder (CuNW) in $TiO_2$ as Photoanode

IOP Conf. Series: Materials Science and Engineering **515** (2019) 012002 doi:10.1088/1757-899X/515/1/012002

# Efficiency Enhancement of Dye-Sensitized Solar Cells (DSSCs) using Copper Nanopowder (CuNW) in $TiO_2$ as Photoanode

**Shahan Shah, N.N.S. Baharun, S.N.F. Yusuf, A.K. Arof***

Centre for Ionics University Malaya, Department of Physics, Faculty of Science, University of Malaya, 50603 Kuala Lumpur, Malaysia.

*Corresponding author's email: akarof@um.edu.my

**Abstract**. The development of renewable energy devices has seen the application of several methods to improve the efficiency of DSSC. One of the methods is to reduce the electron recombination effect from $TiO_2$ to the oxidized dye by introducing copper nanopowder (CuNW) as an electron recombination barrier into the $TiO_2$ layer. The phthaloyl chitosan (PhCh)-based gel polymer electrolytes (GPEs) containing tetrapropylammonium iodide (TPAI) salt, *1*-butyl-*3*-methylimidazolium iodide (BMII) ionic liquid (IL), *4*-tert-butylpyridine (TBP), Guanidinium thiocyanate (GuSCN) as additives and ($I^-/I_3^-$) redox couple have been used as an ion conducting medium in the DSSCs. The DSSCs were characterized by incident photon-to-current conversion efficiency (IPCE) measurements. The DSSC containing 3 wt% of CuNW showed the highest IPCE of 53.7% at 535 nm. Under the irradiation of 1000 W $m^{-2}$ (AM 1.5), 3 wt% of CuNW exhibited the highest cell efficiency, $\eta$ of 7.19%, $J_{sc}$ = 0.0133 A $cm^{-2}$, $V_{oc}$ = 0.76 V, and $FF$ = 0.71.

**Keywords**: Electron recombination barrier, GuSCN, DSSCs, CuNW, $TiO_2$, photoanode.

## 1. Introduction

Dye-sensitized solar cells (DSSCs) were pioneered by O'Regan and Grätzel in 1991 [1]. Since then, DSSC has become a potential photovoltaic device due to their ease of fabrication, economical production and environmentally friendly operation [2-4]. A typical DSSC comprises an iodide-triiodide ($I^-/I_3^-$) redox-based electrolyte, a counter electrode (CE) and dye-sensitized nanocrystalline photoanode,

Under light illumination, excited electrons in the dye-sensitizer conduction band (CB) are injected to the CB of mesoporous semiconductor. The dye is losing an electron during oxidation. In $I^-/I_3^-$ electrolyte, the redox mediator regenerates the oxidized dye producing photocurrent and photovoltage in DSSC [5]. It is clear that an effective and a long-lasting electrolyte plays an important role to transport electron to the oxidized dye from the CE [6]. Gel polymer electrolytes have been introduced to overcome the limitation of liquid electrolytes [7]. A lot of research has also been conducted to improve the DSSCs stability as well as efficiency. According to Chou *et al.* [8], guanidinium thiocyanate (GuSCN) added to the electrolyte improves the performance of DSSCs as guanidinium cations can adsorb onto the oxide semiconductor. The incorporation of GuSCN in the electrolyte can alter the conduction band to a more positive potential. This will lead to the increase in electron injection rate and lead to the enhancement of short circuit current density, $J_{sc}$. Due to the fact that the adsorbed ions will block the recombination sites at the surface of the oxide semiconductor, open circuit voltage, $V_{oc}$ also increases [6,9,10]. Although

DSSCs have reached power conversion efficiency exceeding 12%, its power conversion efficiency for practical application purposes are still low compared to the first generation crystalline-silicon PV cell [11] and second-generation thin-film solar cell [12,13] technologies.

Beside electrolytes, another notable component in DSSC is photoanode. Photoanode consists of nanocrystalline semiconductor that can harness solar energy [3,14,15]. Titanium oxide ($TiO_2$), a wide band gap semiconductor oxide has been widely used in solar cell fabrication. Unfortunately, owing to its large band gap ranging between 3 and 3.2 eV, recombination process can easily occur at the porous $TiO_2$/electrolyte interface [10,16,17]. Various strategies have been conducted to reduce recombination effects in the photoactive $TiO_2$ by incorporation of plasmonic nanostructures with surface plasmon resonance (SPR) [15,18-20]. The addition of plasmonic nanostructures in photovoltaic devices could improve light trapping in the photoactive semiconductor [21]. Noble metals such as silver (Ag), gold (Au), and copper (Cu) were commonly used in plasmonic treatment because they exhibit resonant effect when interacting with visible and ultraviolet photons [22]. Metal nanostructures can be used to scatter incident light within the $TiO_2$ absorbing layer and enhance the $J_{sc}$ and lower the recombination rate [23]. In our previous study, the DSSC cell efficiency increased from 4.61% to 5.21% with $J_{sc}$ of 0.015 A $cm^{-2}$, $V_{oc}$ of 600 mV and $FF$ of 57% after Ag nanoparticles were incorporated in the $TiO_2$ photoanode [24].

In this work, CuNW was introduced to the $TiO_2$ layer so that the charge recombination effect could be controlled [23, 25]. DSSCs were fabricated with $TiO_2$/CuNW sensitized with N3 dye photoanode, GPE containing GuSCN and Pt CE to evaluate the DSSC performance.

## 2. Methods

### *2.1. Materials*

Chitosan, tetrapropylammonium iodide (TPAI), polyethylene oxide (PEO), 4-tert-butylpyridine (TBP), ethylene carbonate (EC), Triton X-100 surfactant, *1*-butyl-*3*-methylimidazolium iodide (BMII), and Guanidinium thiocyanate (GuSCN) were obtained from Sigma-Aldrich. Dimethylformamide (DMF) was obtained from Friedemann Schmidt Chemical. Iodine ($I_2$) crystals and phthalic anhydride were received from Amco-chemie-Humburg. Titanium dioxide ($TiO_2$) particles with the size of 15 nm (P90) and 21 nm (P25) were procured from Evonik Industries. Copper nanoparticles (NW) (60-80 nm) were purchased from Aldrich (Germany). Absolute ethanol was used as a solvent. Cis-diisothiocyanato-bis (2,2'-bipyridyl-4,4'-dicarboxylic acid) ruthenium (II) or N3 dye, and platinum (Pt) solution were received from Solaronix. Carbowax was purchased from Supelco U.S.A.

### *2.2. Preparation of PhCh-PEO-based GPEs*

During phthaloylation, chitosan was reacted with phthalic anhydride and dimethylformamide (DMF) at 120 °C for six hours in a $N_2$ atmosphere. After phthaloylation has occurred, the precipitate was filtered and washed with ethanol for several hours. The drying process took place in a vacuum oven at 60 °C. The product, phthaloyl chitosan (PhCh) was ground finely to prepare GPEs.

The compositions of the GPEs with the various weight percentages of GuSCN are listed in Table 1. PhCh:PEO (4:1) was completely dissolved in DMF and stirred gently for 1 hour at 80 °C until a uniform gel was obtained. TPAI salt, EC plasticizer, TBP, BMII, and different amounts of GuSCN were then added to the gel and stirred continuously until homogenous. Finally, an amount of iodine was added to the GPE at room temperature to form the redox couple.

**Table 1.** The composition of the components in the GPEs in weight percentage (wt%)

| Designation | GuSCN | PEO | PhCh | DMF | EC | TPAI | TBP | BMII | $I_2$ |
|---|---|---|---|---|---|---|---|---|---|
| 0 wt% GuSCN | 0.00 | 1.07 | 4.28 | 26.77 | 32.13 | 19.27 | 7.39 | 7.62 | 1.47 |
| 1 wt% GuSCN | 1.00 | 1.06 | 4.24 | 26.50 | 31.79 | 19.08 | 7.32 | 7.55 | 1.46 |
| 2 wt% GuSCN | 2.00 | 1.05 | 4.20 | 26.24 | 31.49 | 18.89 | 7.25 | 7.47 | 1.41 |
| 3 wt% GuSCN | 3.00 | 1.04 | 4.16 | 26.00 | 31.20 | 18.70 | 7.10 | 7.40 | 1.40 |
| 4 wt% GuSCN | 4.00 | 1.03 | 4.12 | 25.72 | 30.90 | 18.51 | 7.02 | 7.31 | 1.39 |
| 5 wt% GuSCN | 5.00 | 1.02 | 4.10 | 25.48 | 30.68 | 18.30 | 6.85 | 7.21 | 1.36 |

*2.3. Electrochemical Impedance Spectroscopy (EIS) of GPE*

The GPE was sandwiched between two identical stainless-steel electrodes. The diameter of the electrodes was fixed at 2 cm. The GPE impedance measurements were carried out using the HIOKI 3531 Z Hi-Tester from 308 K to 363 K. The range of the frequency measurement was between 50 Hz and 5 MHz. Bulk resistance ($R_b$) of the sample was obtained at the point where the impedance graph intersects the real impedance axis. The ionic conductivity ($\sigma$) of each sample can be then determined using Equation (1):

$$\sigma = \frac{t}{R_b A} \tag{1}$$

here $t$ and A denote the thickness of the sample and contact area of the electrode/electrolyte respectively.

*2.4. Preparation of $TiO_2$/CuNW photoelectrode*

A $TiO_2$ (15 nm) compact layer and another $TiO_2$ (21 nm) porous layer were configured on top of one another. The first $TiO_2$ layer or compact layer was obtained by mixing 0.5 g of $TiO_2$ (P90) powder with 2 mL of nitric acid, $HNO_3$ (molarity, $M$ = 0.1 mol $dm^{-3}$). The mixture was ground for 30 minutes in a mortar until a slurry was obtained. The slurry was then spin coated on the cleaned surface of fluorine doped tin oxide (FTO) glass at 2350 rpm for 60 seconds. The compact layer was then sintered at 450 °C for 30 minutes. The second $TiO_2$ layer (porous $TiO_2$/CuNW) was obtained by grinding the following items: 0.5 g P25 $TiO_2$ powder, 2 mL of 0.1 mol $dm^{-3}$ $HNO_3$ and different weight percentage of copper nanopowder (CuNW), as listed in Table 2. To get a homogeneous paste, 0.1 g carbowax and 1 drop of Triton X-100 surfactant were added. The $TiO_2$/CuNW slurry was then deposited on top of the $TiO_2$ compact layer using the doctor blade method. The electrode was again sintered for 30 minutes at 450 °C. Heating at this temperature also removes the carbowax, thus making the layer porous.

**Table 2.** Designation of different composition of CuNW with $TiO_2$

| Designation | CuNW (g) | $TiO_2$ (g) |
|---|---|---|
| 0 wt% CuNW | 0.000 | 0.500 |
| 1 wt% CuNW | 0.005 | 0.500 |
| 2 wt% CuNW | 0.010 | 0.500 |
| 3 wt% CuNW | 0.015 | 0.500 |
| 4 wt% CuNW | 0.021 | 0.500 |
| 5 wt% CuNW | 0.026 | 0.500 |

The compact and porous $TiO_2$/CuNW layers were sensitized by soaking them in N3 dye dissolved in 10 mL of ethanol. The prepared photoanodes were soaked for 24 hours in the dark at room temperature.

*2.5. Fabrication of Dye-Sensitized Solar Cells (DSSC)*

The highest conducting GPE was used as an electrolyte to assemble DSSCs according to the configuration of FTO/($TiO_2$/CuNW)-dye/GPE/Pt/FTO. The phthaloyl chitosan (PhCh)-based GPE having the composition of PhCh (4.16 wt%), PEO (1.04 wt%), DMF (26.00 wt%), EC (31.20 wt%), TPAI (18.70 wt%), TBP (7.10 wt%), BMII (7.40 wt%), GuSCN (3.00 wt%), and $I_2$ (1.40 wt%) was used as an ion conductor in the DSSC. The counter electrode (CE) was prepared by drop casting plastisol (Solaronix) onto the FTO glass until it covered the entire surface. The electrode was sintered for 30 minutes at 450 °C.

The effects of photocurrent density ($J$) on voltage ($V$) of the DSSCs were measured using a Keithley 2400 electrometer. The measurement was carried out under irradiation intensity of 1000 W $m^{-2}$. The solar cell's active area is 0.20 $cm^2$. Equation (2) below was used to calculate the fill factor ($FF$):

$$FF = \frac{J_{\max} \times V_{\max}}{J_{sc} \times V_{oc}} \tag{2}$$

where the maximum current density is $J_{max}$ and the maximum voltage is $V_{max}$. $J_{sc}$ is the short-circuit current density and $V_{oc}$ is the open-circuit voltage. The following Equation (3) was used to obtain power conversion efficiency ($\eta$):

$$\eta(\%) = \frac{V_{oc} \times J_{sc} \times FF}{P_{in}} \times 100\% \tag{3}$$

where $P_{in}$ is incident light power density.

IPCE measurements were operated using a Newport Model 70528 Oriel Monochromator Illuminator. The incident photon to current conversion efficiency value demonstrates the amount of current produced by the cell as it was irradiated by photons in the wavelength range studied.

## 3. Results and Discussion

*3.1. The Addition of guanidinium thiocyanate in polymer electrolytes*

Guanidinium thiocyanate (GuSCN) was added to the PhCh-PEO-EC-TPAI-BMII-TBP-$I_2$ gel polymer electrolytes. Previous studies have proven that GuSCN influenced the electron injection yield due to the shifting of $TiO_2$ flat band potential. This will lead to the increment of $J_{SC}$ and also the efficiency of DSSCs [10,26-28]. The effects of GuSCN concentration onto the ionic conductivity of PhCh-PEO-based GPEs at room temperature are shown in Table 3. After the addition of 1 wt% GuSCN to the GPE system, the ionic conductivity obtained was $11.35 \times 10^{-3}$ S $cm^{-1}$. The further increment can be observed as more GuSCN introduced that it contributed to a high number density of free charges. The maximum ionic conductivity was achieved by the GPE containing 3 wt% GuSCN with the value of $12.69 \times 10^{-3}$ S $cm^{-1}$. Beyond this concentration, the ionic conductivity began to decrease. This might be due to the lesser free ion concentration because of the formation of neutral ion pairs that do not contribute to conductivity. Therefore, in this work, DSSCs were fabricated using the optimized GPE with 3 wt% GuSCN content. Temperature dependence conductivities from 308 K to 363 K for electrolyte containing 3 wt% of GuSCN are shown in Figure 1. The conductivity-temperature data were fitted to Arrhenian characteristics from 308 K to 363 K within temperature range studied.

**Table 3.** Ionic conductivity values at room temperature for GPEs with various contents of GuSCN.

| GuSCN content (wt%) | Conductivity, $\sigma$ (mS cm$^{-1}$) |
|---|---|
| 1 | 11.35 |
| 2 | 12.49 |
| 3 | 12.69 |
| 4 | 11.29 |
| 5 | 10.56 |

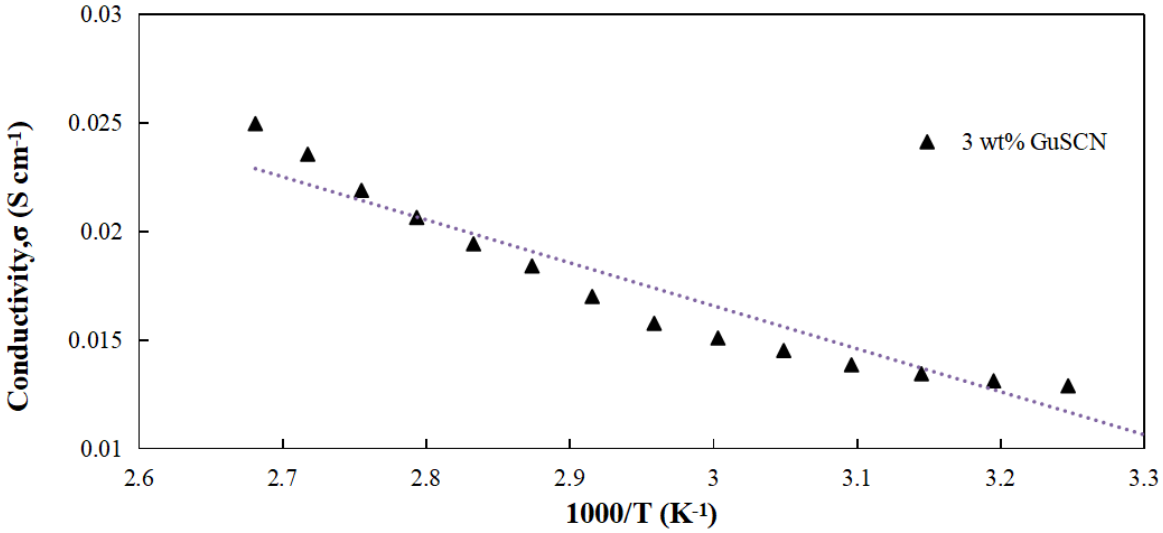


**Figure 1.** The conductivity-temperature relationship for the gel polymer electrolytes with 3 wt% GuSCN content

*3.2. J-V Characteristics of DSSCs*

Figure 2 displays the *J–V* characteristics of the fabricated DSSCs. The photoanodes each contained various wt% of CuNW. The most conducting GPE with 3 wt% of GuSCN was used in the fabrication of DSSCs. The corresponding parameters that can be obtained from the *J-V* characteristics are listed in Table 4. The DSSC fabricated with 0 wt% of CuNW photoanode exhibited a comparatively low solar cell efficiency value of 4.62% with $J_{sc}$ of 9.57 mA cm$^{-2}$ and $V_{oc}$ of 0.72 V. After 1 wt% of CuNW was added, the DSSC efficiency value was observed to increase to 5.41%. It can be observed that the efficiency of DSSC with 2 wt% of CuNW further increased to 6.32%. On addition of 3 wt% CuNW, the highest value of $J_{sc}$, $V_{oc}$, *FF* and efficiency were obtained with 13.33 mA cm$^{-2}$, 0.76 V, 0.71 and 7.19%, respectively. The efficiency improvement indicated that CuNW has prevented electrons from oxidized dye molecules to recombine with the redox mediator in the electrolyte. This is evident from the increased $J_{sc}$ (up to 3 wt% CuNW) in Table 4. This relationship can also be observed in Figure 3 where the $J_{sc}$ value increases with increasing of CuNW content, parallel to the efficiency value of the cells.

The performance of the cells dropped at higher concentration of CuNW (4 and 5 wt%). This could be due to the much thicker $TiO_2$/CuNW that is inserted on the layer. The addition of certain amount of CuNW might cause a metal bulk effect [29]. As Cu has high work function, they exhibited strong bulk effect. According to Hailing *et al.* [29], higher amount of metal loading lead to the bigger size of cluster, which degraded the performance of the DSSC. The DSSC efficiency increased with 5 to 20 s electroplating time at 10 mA current, but decreased using 25 and 40 s electroplating time [30]. The presence of excessive Cu may also inhibit the working process of $TiO_2$ thus lower the performance of the cells [31].

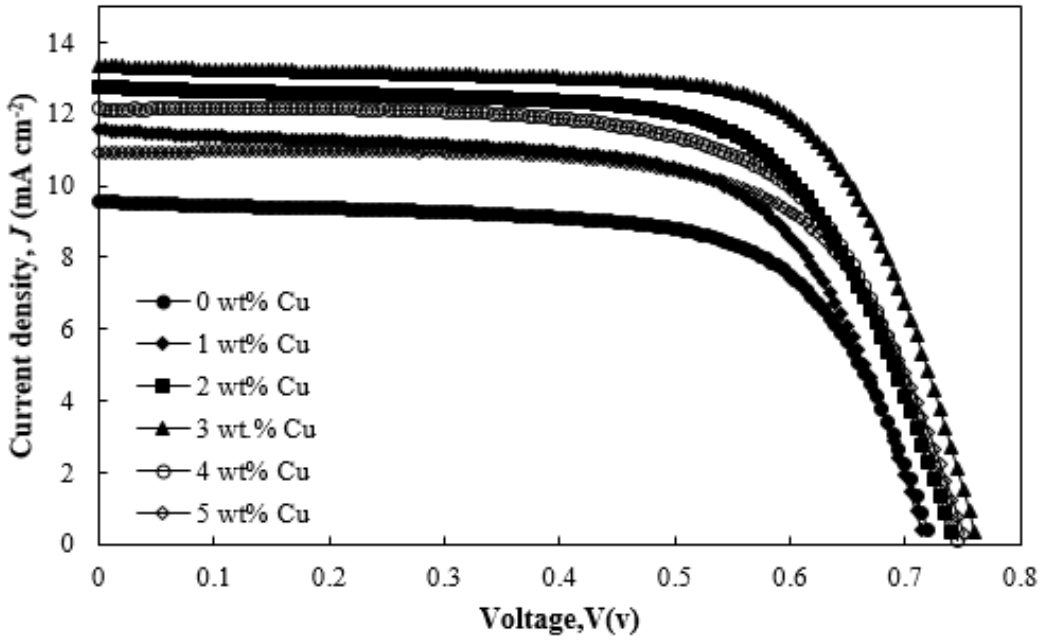


**Figure 2.** *J-V* characteristics of DSSC with various content of CuNW

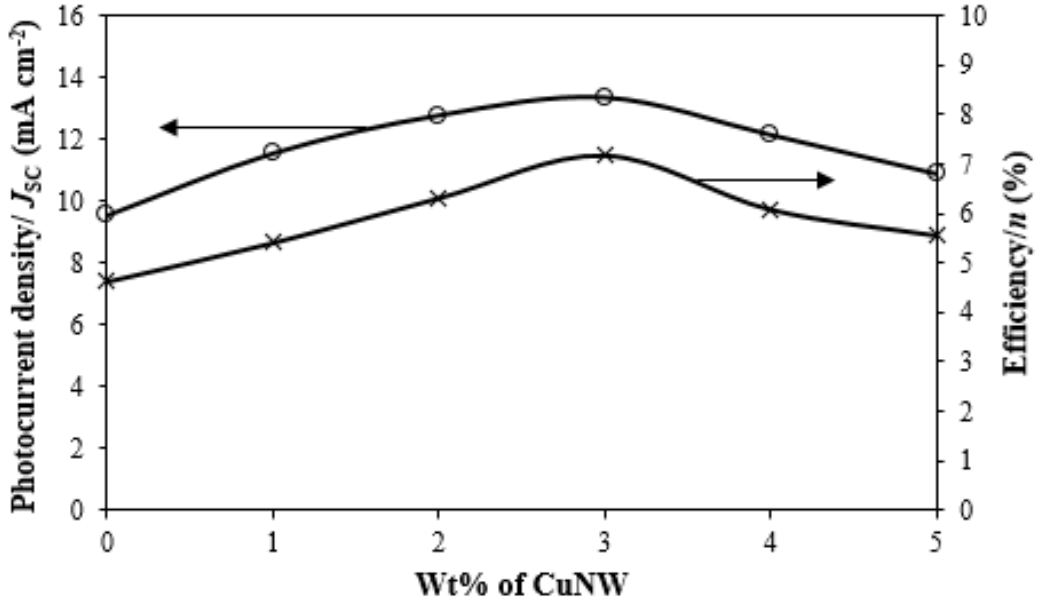


**Figure 3.** Variation of photocurrent density and efficiency of DSSCs with different wt% of CuNW

Figure 4 shows the method of estimating shunt resistance ($R_{sh}$) and series resistance ($R_s$) from *J-V* characteristics. $R_{sh}$ and $R_s$ can be obtained from the inverse slope from its linear part of the $J_{sc}$ and $V_{oc}$, respectively. Table 4 listed the value of $R_{sh}$ and $R_s$ calculated from this method. $R_s$ and $R_{sh}$ play a major role in controlling the value of fill factor, *FF* [32] . According to Table 4, DSSC with 3 wt% of CuNW possess highest $R_{sh}$ and also lowest $R_s$ which correspond to the highest value of *FF*. Similar observation was reported by Zhang *et al.* [33].

**Table 4.** Effects of CuNW to the DSSC parameters

| CuNW content (wt%) | $J_{sc}$ (mA cm$^{-2}$) | $V_{oc}$ (V) | *FF* | $\eta$ (%) | $R_{sh}$ (Ω cm$^2$) | $R_s$ (mΩ cm$^2$) |
|---|---|---|---|---|---|---|
| 0.00 | 9.57 | 0.72 | 0.62 | 4.62 | 0.72 | 12.90 |
| 1.00 | 11.55 | 0.71 | 0.66 | 5.41 | 0.79 | 11.10 |
| 2.00 | 12.76 | 0.74 | 0.67 | 6.32 | 1.22 | 10.50 |
| 3.00 | 13.33 | 0.76 | 0.71 | 7.19 | 1.35 | 10.40 |
| 4.00 | 12.14 | 0.74 | 0.67 | 6.09 | 1.20 | 10.90 |
| 5.00 | 10.90 | 0.75 | 0.68 | 5.56 | 1.14 | 12.30 |

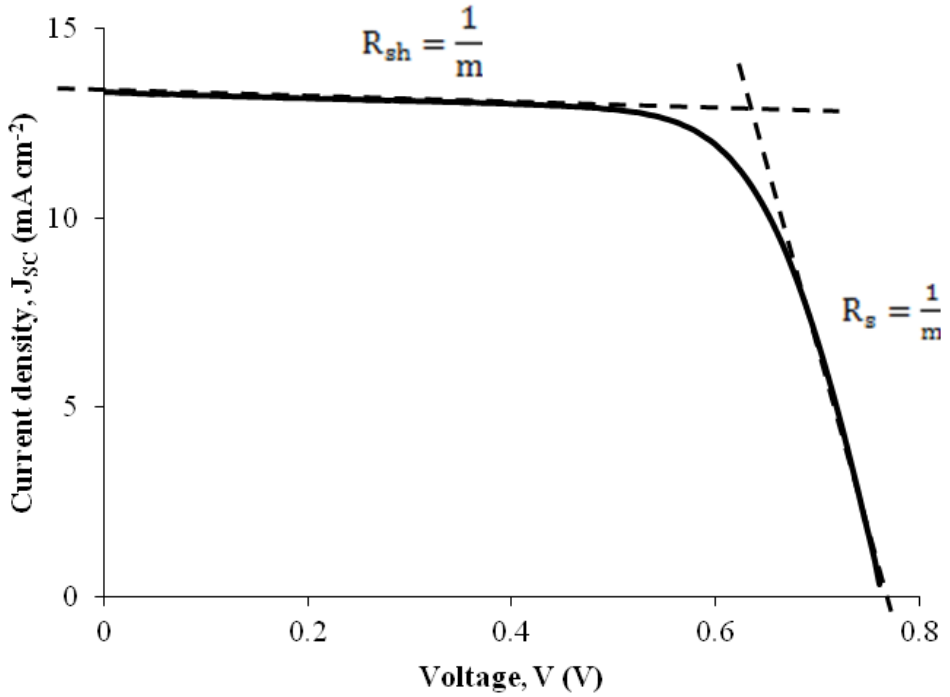


**Figure 4.** Estimating $R_{sh}$ and $R_s$ from *J-V* characteristics

*3.3. IPCE*

The plots of IPCE versus wavelength of the cells containing various amounts of CuNW are shown in Figure 5 and the data is tabulated in Table 5. IPCE measurements were done to understand the photocurrent generation of the cell based on different characteristics of $TiO_2$ photoanode. The IPCE result was observed to be parallel with the $J_{SC}$ values shown in the previous section. The percentage of the IPCE achieved by the cells increased as the CuNW content increased. The most efficient DSSC in this system containing 3 wt% CuNW also obtained the highest IPCE% value of 53.70% at 535 nm wavelength. At higher content of CuNW, the percentage of the IPCE decreases. According to Subramanian *et al.* [34], the improvement of the DSSC performance might be due to the enhancement of charge injection and photocurrent, since the $TiO_2$ photoanode conduction band edge shifted downwards. Thus, the electron recombination in the electrolyte reduced and efficiency increases.

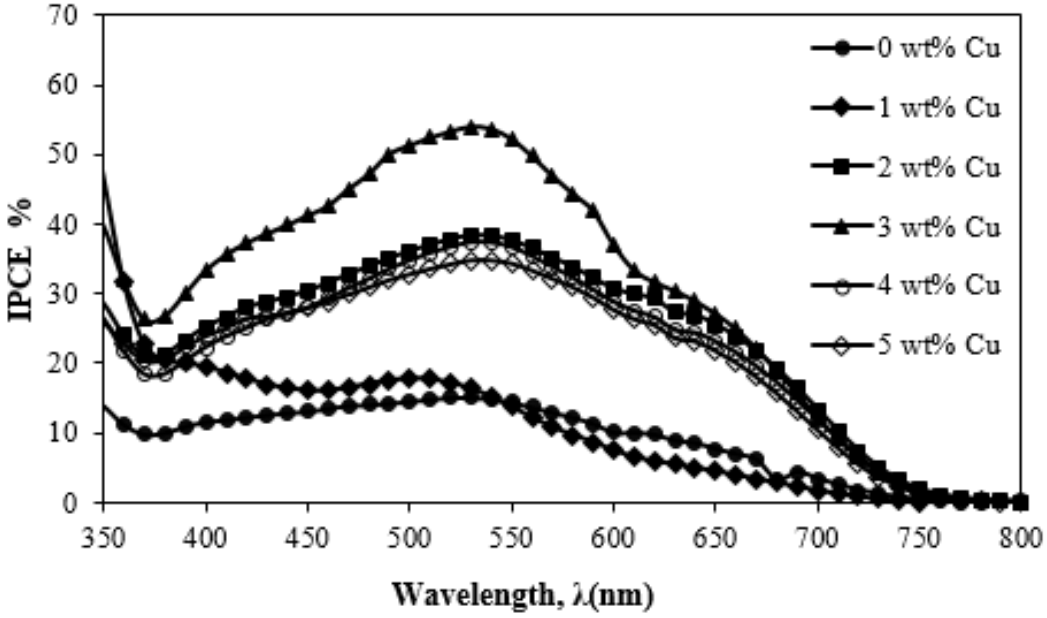


**Figure 5.** IPCE plot of the $TiO_2$/CuNW based DSSCs

**Table 5.** IPCE (%) of DSSCs with different amount of CuNW

| CuNW content (wt%) | IPCE (%) | Wavelength(nm) |
|---|---|---|
| 0 | 15.01 | 540 |
| 1 | 17.71 | 500 |
| 2 | 38.30 | 530 |
| 3 | 53.70 | 535 |
| 4 | 37.30 | 540 |
| 5 | 34.80 | 535 |

## 4. Conclusion

CuNW have proved to be one of the efficient additives in $TiO_2$ photoanode layer to reduce the electron recombination rate in DSSCs. Solar cell with 3 wt% of CuNW gave the best performance with the value of 7.19%, and is higher compared to the sample without CuNW (4.62%). IPCE measurements also obtained the similar observation as $TiO_2$ layer containing 3 wt% of CuNW achieved the highest percentage of 53.70% at wavelength 535 nm. The DSSC fabricated with this efficient electrolyte also exhibited the highest shunt resistance and lowest serial resistance.

## References

[1] O'Regan B and Gratzel M, *A low-cost, high-efficiency solar cell based on dye-sensitized colloidal $TiO_2$ films.* Nature, 1991. **353**(6346): p. 737-740.
[2] Grätzel M, *Recent advances in sensitized mesoscopic solar cells.* Accounts of Chemical Research, 2009. **42**(11): p. 1788-1798.
[3] Grätzel M, *Photoelectrochemical cells.* Nature, 2001. **414**: p. 338.
[4] Hagfeldt A, Boschloo G, Sun L, Kloo L, and Pettersson H, *Dye-sensitized solar cells.* Chem Rev, 2010. **110**(11): p. 6595-663.

[5] Li L-L, Chang Y-C, Wu H-P, and Diau EW-G, *Characterisation of electron transport and charge recombination using temporally resolved and frequency-domain techniques for dye-sensitised solar cells.* International Reviews in Physical Chemistry, 2012. **31**(3): p. 420-467.
[6] Jena A, Mohanty SP, Kumar P, Naduvath J, Gondane V, Lekha P, Das J, Narula HK, Mallick S, and Bhargava P, *Dye Sensitized Solar Cells: A Review.* Transactions of the Indian Ceramic Society, 2012. **71**(1): p. 1-16.
[7] Aziz SB, Woo TJ, Kadir MFZ, and Ahmed HM, *A conceptual review on polymer electrolytes and ion transport models.* Journal of Science: Advanced Materials and Devices, 2018. **3**(1): p. 1-17.
[8] Chou C-Y, Lee C-P, Vittal R, and Ho K-C, *Efficient quantum dot-sensitized solar cell with polystyrene-modified TiO2 photoanode and with guanidine thiocyanate in its polysulfide electrolyte.* Journal of Power Sources, 2011. **196**(15): p. 6595-6602.
[9] Wu J, Lan Z, Lin J, Huang M, Huang Y, Fan L, and Luo G, *Electrolytes in Dye-Sensitized Solar Cells.* Chemical Reviews, 2015. **115**(5): p. 2136-2173.
[10] Zhang C, Huang Y, Huo Z, Chen S, and Dai S, *Photoelectrochemical Effects of Guanidinium Thiocyanate on Dye-Sensitized Solar Cell Performance and Stability.* The Journal of Physical Chemistry C, 2009. **113**(52): p. 21779-21783.
[11] Zhao J, Wang A, and Green MA, *High-efficiency PERL and PERT silicon solar cells on FZ and MCZ substrates.* Solar Energy Materials and Solar Cells, 2001. **65**(1): p. 429-435.
[12] Saliba M, Orlandi S, Matsui T, Aghazada S, Cavazzini M, Correa-Baena J-P, Gao P, Scopelliti R, Mosconi E, Dahmen K-H, De Angelis F, Abate A, Hagfeldt A, Pozzi G, Graetzel M, and Nazeeruddin MK, *A molecularly engineered hole-transporting material for efficient perovskite solar cells.* Nature Energy, 2016. **1**: p. 15017.
[13] Repins I, Contreras MA, Egaas B, DeHart C, Scharf J, Perkins CL, To B, and Noufi R, *19·9%-efficient ZnO/CdS/CuInGaSe$_2$ solar cell with 81·2% fill factor.* Progress in Photovoltaics: Research and Applications, 2008. **16**(3): p. 235-239.
[14] Ako RT, Ekanayake P, Young DJ, Hobley J, Chellappan V, Tan AL, Gorelik S, Subramanian GS, and Lim CM, *Evaluation of surface energy state distribution and bulk defect concentration in DSSC photoanodes based on Sn, Fe, and Cu doped TiO$_2$.* Applied Surface Science, 2015. **351**: p. 950-961.
[15] Dhonde M, Sahu K, Murty VVS, Nemala SS, and Bhargava P, *Surface plasmon resonance effect of Cu nanoparticles in a dye sensitized solar cell.* Electrochimica Acta, 2017. **249**: p. 89-95.
[16] Grätzel M, *Dye-sensitized solar cells.* Journal of Photochemistry and Photobiology C: Photochemistry Reviews, 2003. **4**(2): p. 145-153.
[17] Subramanian V, Wolf E, and Kamat PV, *Semiconductor−Metal Composite Nanostructures. To What Extent Do Metal Nanoparticles Improve the Photocatalytic Activity of TiO$_2$ Films?* The Journal of Physical Chemistry B, 2001. **105**(46): p. 11439-11446.
[18] Catchpole KR and Polman A, *Plasmonic solar cells.* Optics Express, 2008. **16**(26): p. 21793-21800.
[19] Wu JL, Chen FC, Hsiao YS, Chien FC, Chen PL, Kuo CH, Huang MH, and Hsu CS, *Surface Plasmonic Effects of Metallic Nanoparticles on the Performance of Polymer Bulk Heterojunction Solar Cells.* Acs Nano, 2011. **5**(2): p. 959-967.
[20] Nakayama K, Tanabe K, and Atwater HA, *Plasmonic nanoparticle enhanced light absorption in GaAs solar cells.* Applied Physics Letters, 2008. **93**(12): p. 3.
[21] Ferry VE, Munday JN, and Atwater HA, *Design Considerations for Plasmonic Photovoltaics.* Advanced Materials, 2010. **22**(43): p. 4794-4808.
[22] Linic S, Christopher P, and Ingram DB, *Plasmonic-metal nanostructures for efficient conversion of solar to chemical energy.* Nature Materials, 2011. **10**(12): p. 911-921.
[23] Park J-Y, Kim C-S, Okuyama K, Lee H-M, Jang H-D, Lee S-E, and Kim T-O, *Copper and nitrogen doping on TiO$_2$ photoelectrodes and their functions in dye-sensitized solar cells.* Journal of Power Sources, 2016. **306**: p. 764-771.

[24] Shah S, Noor IM, Pitawala J, Albinson I, Bandara TMWJ, Mellander BE, and Arof AK, *Plasmonic effects of quantum size metal nanoparticles on dye-sensitized solar cell.* Optical Materials Express, 2017. **7**(6): p. 2069-2083.
[25] Nissfolk J, Fredin K, Hagfeldt A, and Boschloo G, *Recombination and Transport Processes in Dye-Sensitized Solar Cells Investigated under Working Conditions.* The Journal of Physical Chemistry B, 2006. **110**(36): p. 17715-17718.
[26] Grätzel M, *Conversion of sunlight to electric power by nanocrystalline dye-sensitized solar cells.* Journal of Photochemistry and Photobiology A: Chemistry 2004. **164** p. 3–14.
[27] Wang Y, Lu J, Yin J, Lü G, Cui Y, Wang S, Deng S, Shan D, Tao H, and Sun Y, *Influence of 4-tert-butylpyridine/guanidinium thiocyanate co-additives on band edge shift and recombination of dye-sensitized solar cells: Experimental and theoretical aspects.* Electrochimica Acta, 2015. **185**: p. 69–75.
[28] Jeanbourquin XA, Li X, Law C, Barnes PRF, Humphry-Baker R, Lund P, Asghar MI, and O'Regan BC, *Rediscovering a key interface in dye-sensitized solar cells: Guanidinium and iodine competition for binding sites at the dye/electrolyte surface.* Journal of the American Chemical Society, 2014. **136**(20): p. 7286–7294.
[29] Zhu H, Zhang J, Wang T, Wang L, Lan X, and Huang B, *Photocatalytic performance of $TiO_2$ thin films connected with Cu micro-grid.* Science in China Series E: Technological Sciences, 2009. **52**(8): p. 2175-2179.
[30] Rokhmat M, Wibowo E, Sutisna, Khairurrijal, and Abdullah M, *Performance Improvement of $TiO_2$/CuO Solar Cell by Growing Copper Particle Using Fix Current Electroplating Method.* Procedia Engineering, 2017. **170**: p. 72-77.
[31] Rokhmat M, Wibowo E, Sutisna, Khairurrijal, and Abdullah M, *Development of a low-cost $TiO_2$/CuO/Cu solar cell by using combined spraying and electroplating method.* J. Math. Fund. Sci., 2018. **50**(1): p. 92-101.
[32] Qi BY and Wang JZ, *Fill factor in organic solar cells.* Physical Chemistry Chemical Physics, 2013. **15**(23): p. 8972-8982.
[33] Zhang J, Lee S-T, and Sun B, *Effect of Series and Shunt Resistance on Organic-Inorganic Hybrid Solar Cells Performance.* Electrochimica Acta, 2014. **146**: p. 845-849.
[34] Subramanian A, Ho C-Y, and Wang H, *Investigation of various photoanode structures on dye-sensitized solar cell performance using mixed-phase $TiO_2$.* Journal of Alloys and Compounds, 2013. 572: p. 11-16.

**Acknowledgements**
The authors acknowledge the financial support from the Malaysian Ministry of Higher Education in the form of Fundamental Research Grant Scheme (FRGS) under project No. FG029-17AFR